ELSEVIER

Deep-Sea Research II 52 (2005) 2911–2927

DEEP-SEA RESEARCH
PART II

www.elsevier.com/locate/dsr2

The fate of phosphate in an in situ Lagrangian addition experiment in the Eastern Mediterranean

C.S. Law[a,b,*], E.R. Abraham[b], E.M.S. Woodward[a], M.I. Liddicoat[a], T.W. Fileman[a], T.F. Thingstad[c], V. Kitidis[a,d], T. Zohary[e]

[a]*Plymouth Marine Laboratory, Prospect Place, Plymouth, UK*
[b]*National Institute for Water and Atmospheric Research (NIWA), Private Bag 14-901, Evans Bay Parade, Kilbirnie, Wellington, New Zealand*
[c]*Department of Biology, University of Bergen, Bergen, Norway*
[d]*School of Marine Science and Technology, University of Newcastle, Newcastle-Upon-Tyne, UK*
[e]*Israel Oceanographic Limnological Research, Kinneret Limnological Laboratory, Tiberias, Israel*

Accepted 16 August 2005

Abstract

The Eastern Mediterranean is the largest oceanic ecosystem that is phosphate-limited. To determine the impact of a transient input we executed a phosphate addition experiment in the surface waters of the Cyprus Eddy (33.3°N 32.3°E), and compared the ecosystem response with surrounding unperturbed water. A tracer, sulphur hexafluoride (SF_6), added with the phosphate, enabled tracking of the patch when phosphate concentration declined to detection limits, and provided quantitative estimates of mixing, dilution and patch volume. The patch expanded to $>400\,km^2$ over 9 days with a lateral diffusion rate of $23\pm2\,m^2/s$ that was consistent with previous tracer releases in eddies. Mixed layer phosphate concentration was ~110 nmol/l immediately post-release, and declined to <5 nmol/l after 6 days. A phosphate budget was developed using SF_6 as a proxy to discriminate between dilution and biological pathways, with dilution resulting in loss of ~75% of added phosphate from the patch centre by day 3. Non-conservative phosphate loss was largely due to biological incorporation into particulate-P, of which 50% accumulated at the patch centre whilst the remainder was removed by lateral dilution by day 3. Non-conservative phosphate loss at the patch centre was 15–15.5 nmol/l by day 4, which was equal to the cumulative biological P uptake of 15.6 (±5.6) nmol/l P and concurred with two other independent estimates of P uptake. This closure of the phosphate budget infers that the transfer of added P to mesozooplankton and higher consumers was not significant within the timescale of the experiment, despite the observed biomass increase that followed phosphate addition. Although patch dilution significantly reduced phosphate concentration and particulate accumulation, and so the apparent biological response to the added phosphate, analysis suggests that lateral mixing would not prevent bacterial biomass accumulation at the growth rates observed, suggesting that another factor such as grazing was responsible.

Keywords: Dilution; Phosphate; Phytoplankton; Bacteria; Eastern Mediterranean; Phosphate enrichment; Diffusion

*Corresponding author. National Institute for Water and Atmospheric Research (NIWA), Private Bag 14-901, Evans Bay Parade, Kilbirnie, Wellington, New Zealand. Tel.: +64 43860478; fax: +64 43862153.
E-mail address: c.law@niwa.co.nz (C.S. Law).

0967-0645/$ - see front matter © 2005 Elsevier Ltd. All rights reserved.
doi:10.1016/j.dsr2.2005.08.017

1. Introduction

The Eastern Mediterranean is an ultra-oligotrophic body of water that is recognised as the largest open ocean region in which primary production is limited by phosphate availability (Krom et al., 1991). Phosphate and nitrate in surface waters are extremely low during spring-summer, and this is reflected in low phytoplankton biomass, with chlorophyll *a* at less than 0.5 mg m^{-3} (Krom et al., 2005; Psarra et al., 2005). Over winter surface water nutrients are replenished by deep mixing with Levantine Intermediate Water that has an inorganic N:P ratio of 29. As this represents the primary source of nutrients for autotrophic production it is perhaps not surprising that, following biological uptake, excess dissolved inorganic nitrogen remains (0.5–1 μmol/l), whereas phosphate is undetectable using conventional micromolar analytical techniques (Krom et al., 1992, 2003). Phosphate limitation during late winter-spring has also been inferred from microcosm experiments which have shown increases in phosphate uptake and phytoplankton biomass upon phosphate addition or combined phosphate and nitrate additions, but not with nitrate addition alone (Bonin et al., 1989). Phytoplankton and heterotrophic bacterial production were also shown to be P-limited during winter in both the Levantine Basin and Cretan Sea (Zohary and Robarts, 1998; Christaki et al., 2001). The presence of Alkaline Phosphatase, an enzyme produced in response to low phosphate, is further evidence of physiological P limitation in spring (Thingstad and Mantoura, 2005). However, the situation appears more equivocal in summer, when the absence of both nitrate and phosphate in surface waters, and the observed biological response to addition of either nutrient in microcosm experiments, suggests seasonal co-limitation (Krom et al., 2003; Zohary et al., 2005).

The uncertainty regarding P limitation, or N and P co-limitation, makes it difficult to predict how the Eastern Mediterranean will respond to chronic or acute change in nutrient supply. Allochthonous nutrient sources in the Eastern Mediterranean to the coastal margins include aeolian deposition, terrestrial run-off, mariculture and sewage outfalls, although the impact of the latter examples is localised. The region receives significant dust deposition originating from the Sahara, which has been identified as both a potential sink (Krom et al., 1991), and source of N and P (Carbo et al., 2005; Herut et al., 1999, 2005). Climate change may potentially result in variability in wind mass trajectory and aridification that may alter both the composition, and the frequency and duration of aeolian input to the E. Mediterranean (Carbo et al., 2005), with potential implications for microbial community structure and productivity. Aeolian dust input currently maintains availability of the micronutrient iron in the Eastern Mediterranean at levels that exceed the global average for the open ocean (Krom et al., 2003), which may influence nitrogen fixation in this region (Gruber and Sarmiento, 1997). Climate forcing may also influence nutrient supply to the Eastern Mediterranean via water mass circulation. Recent reported changes in deep water formation (Roether et al., 1996) indicate increased upward mixing in the Levantine basin and shoaling of the nutricline (Klein et al., 1999), which may alter long term productivity and community composition.

Although the Eastern Mediterranean is highly vulnerable to change, the ecosystem response to variation in nutrient supply has received little attention. This is in contrast to other regions such as high nitrate low chlorophyll (HNLC) waters, in which ecosystem response to the limiting micronutrient, iron, is well documented. Increases in iron availability in HNLC waters generally stimulates a strong response in the larger autotrophs, with significant biomass accumulation by diatoms (Boyd et al., 2000), whereas the response of the heterotrophic and autotrophic picoplankton is limited by microzooplankton grazing (Hall and Safi, 2001). However, in contrast to HNLC waters, heterotrophic bacteria and phytoplankton biomasses are of similar magnitude in low nutrient low chlorophyll (LNLC) regions such as the Eastern Mediterranean (Pitta et al., 2005; Li et al., 1992). In addition, the potential for N and P co-limitation, or switching of limiting nutrient when the other is available, confirms that HNLC regions are not appropriate models for LNLC regions. Although our current understanding of nutrient limitation in the E. Mediterranean is primarily based upon microcosm experiments (Bonin et al., 1989; Zohary and Robarts, 1998), the observations from such experiments may not reflect the in situ response due to artefacts such as exclusion of larger consumers, altered cycles of light, mixing and turbulence, surface effects and potential nutrient contamination (Banse, 1991). Mesoscale in situ addition experiments have successfully overcome the limitations of

small-scale incubations in HNLC regions, and conclusively demonstrated the iron hypothesis (Martin et al., 1994; Boyd et al., 2000). Furthermore they have provided insight into associated aspects of the biogeochemistry and fate of algal blooms that could not be achieved at the scale of microcosm incubations (Boyd et al., 2004). Whereas the iron addition required for a mesoscale experiment in HNLC waters is logistically achievable due to the low phytoplankton requirement (Fe:C of 10^{-5}–10^{-6}), a mesoscale in situ phosphate addition in a LNLC region presents more of a challenge, as it requires considerably greater quantities of phosphate to alleviate physiological P limitation and stimulate a measurable response. Recent advances in both addition technology and analytical capabilities have overcome this limitation and increased the viability of an in situ addition experiment to establish the controls on ecosystem productivity and structure in the Eastern Mediterranean. This paper details the execution and evolution of the first in situ oceanic phosphate addition experiment (CYCLOPS) in the Cyprus Eddy, an anti-cyclonic warm-core eddy in the S. E. Levantine Basin (Zodiatis et al., 2005). We describe the physical evolution of the enriched patch and the application of sulphur hexafluoride, SF_6, which provided a proxy for the added phosphate and a tracer of mixing, dilution and patch volume (Law et al., 1998, 2001; Abraham et al., 2000). This provided a physical context for interpretation of phosphate dynamics, with discrimination between dilution and non-conservative phosphate removal, with generation of a phosphate budget and determination of the fate of the added phosphate.

2. Methods

2.1. Phosphate and tracer release

The phosphate solution was prepared prior to sailing at Limmasol, Cyprus, by adding concentrated phosphoric acid, with sodium bicarbonate to buffer pH, to nutrient-depleted seawater (M. Krom, pers. comm.). This was carried out in 6×3000 l tanks, with a final concentration of 2.2 M dissolved inorganic orthophosphate. The experiment was undertaken from the R/V *Aegaeo* in the Cyprus Eddy on 17–27 May 2002 (Fig. 1A). Initially the area was surveyed to identify the position of the eddy centre (Zodiatis et al., 2005), and establish the variability in biological and biogeochemical parameters prior to the release. The nominal centre of the eddy, as identified from the CTD survey, was marked by a drifter buoy equipped with a GPS transmitter that updated its position at 10-min intervals via UHF uplink to the ship. SF_6 saturation of surface water was achieved during the release using an in-line saturation unit in which surface water was continuously sprayed through an atmosphere of pure SF_6. Saturation efficiency was monitored at 10-min intervals by collection of 50 ml water samples downstream of the in-line system, followed by static equilibration with an equal volume of Helium and analysis by TCD-GC, and remained relatively uniform at ~44% throughout. The SF_6 solution was mixed with the phosphate solution using a dual pumping system, with flow rates of ~850 l/h for the SF_6 solution and ~2700 l/h for the phosphate solution. The output rate of the phosphate tanks was balanced to ensure uniform release, with the combined phosphate/SF_6 solution pumped to a depth of 9–11 m in a 16 m surface mixed layer. Approximately 39 000 M of phosphate solution and 0.44 M of SF_6 were released with a molar release ratio of ~90 000. The release was coordinated in a Lagrangian framework by reference to the GPS drifter buoy which was drogued at a depth of ~10 m to ensure that it was advected with the surface mixed layer. The release took 6.5 h at a ship's speed of ~5 knots, during which the drifter buoy moved initially north-west and then north-east. The release ship track described an expanding hexagon around the buoy (Fig. 1B) with post-release Lagrangian correction confirming that it was primarily within an area of 2×2 km over a total area of ~16 km^2 (Fig. 1C). The mid-point of the release at 1200 GMT 17/5/02 was used as the reference time zero (T0) for the experiment.

2.2. Underway surface SF_6 mapping

Surface mapping of the patch began on 18/05/02, following a 6-h period to allow the SF_6 and phosphate to disperse into the surface mixed layer. Surface water was pumped from the ship's intake to the mapping system, in which dissolved SF_6 was continuously sparged, trapped cryogenically, separated chromatographically from oxygen, and quantified by ECD-GC (Law et al., 1998). A [SF_6] measurement was obtained every 3 minutes, time- and position-stamped by GPS, and incorporated into a real-time visualisation of surface [SF_6] relative to the ship's position in Earth coordinates.

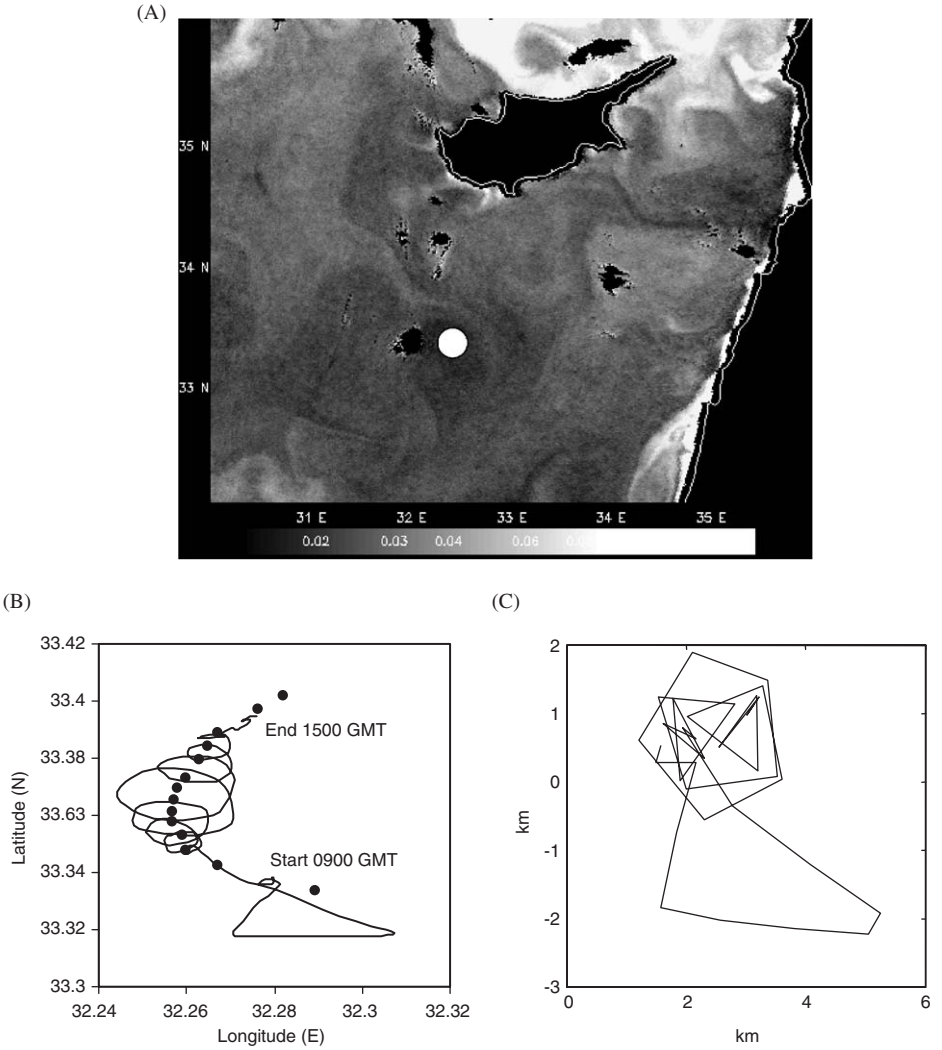

Fig. 1. (A) Ocean colour image of the Eastern Mediterranean with the white circle indicating the position of the Cyprus Eddy, (B) the ships track (solid line) and GPS buoy positions (dots) in earth coordinates during the phosphate/SF_6 release on 17 May 2002 and (C) ships track during the release following Lagrangian correction by reference to the GPS buoy (0, 0).

Surface [SF_6] distribution was mapped for 9 days, during which concentration declined as the patch mixed with surrounding water and SF_6 was lost to the atmosphere. The patch was mapped on a daily basis at a ship speed of 7–10 knots for periods of 8–11 h overnight, although sub-surface [SF_6] distribution was mapped by continuous pumping from a depth of 12–14 m on 20/05/02. A Lagrangian correction was subsequently applied to the [SF_6] data post-cruise using the relative position of the drifter buoy as a reference for each sample. The patch centre was identified from the mapping data at the end of each mapping session, and vertical profiling carried out at the selected IN station. On every other day the ship moved to a minimum distance of 15 km from the patch centre for vertical profiling at an OUT station. Water column profiles were obtained by CTD hydrocast at both IN and OUT stations, with discrete [SF_6] analysis on 350 ml water samples using a technique similar to the mapping, but with the inclusion of a vacuum-sparging step (Law et al., 1994).

2.3. Nutrient measurement

Phosphate concentration [DIP] was measured with a detection limit of 2 nmol/l, using a recently developed sea-going analytical technique (Woodward

and Kitidis, unpublished) incorporating a 2-m liquid wave guide capillary cell as the flow-cell and an optimised segmented flow colorimetric analysis technique (Woodward and Rees, 2001, 2002). This was operated during the experiment in both underway mode from the pumped on-line sea-water supply, and in discrete sample mode using CTD hydrocasts and point sampling (Krom et al., 2005). Micromolar analysis was also carried out for phosphate using a 5-channel Technicon segmented flow autoanalyser. Samples were analysed within 2 h of sample collection, and clean sample handling techniques were employed to avoid contamination. The micromolar procedures are quality controlled and monitored by participation in the international QUASIMEME intercalibration programme.

3. Results

3.1. Lateral evolution of the patch

The Cyprus Eddy is a permanent quasi-stationary eddy that is the primary feature of the general circulation of the S.E. Levantine Basin. The eddy core was characterised by a temperature of ~17.25 °C and salinity 39.1 psu, and was isothermal from ~100 to 280 m during CYCLOPS (Krom et al., 2005). Surface currents were minimal at the eddy centre, and increased to a maximum of 35–45 cm/s at the northern periphery (Zodiatis et al., 2005). The GPS drifter buoy was transported anti-cyclonically around the eddy centre and exhibited inertial oscillations with a period of ~24 h and a low-frequency rotation with a period of ~1 week (Fig. 2). The drifter buoy remained within the SF_6 patch for the duration of the 9-day experiment and circumnavigated a central point at an arc distance of ~3 nmiles, confirming that the eddy centre was at 33.27°N 32.36°E.

Concurrent surface mapping of [DIP] and [SF_6] was only carried out on days 1 and 2 (Fig. 3). The mean initial [DIP]:[SF_6] ratio at the patch centre during the first mapping session was ~92 000, consistent with the estimated molar ratio from the release. [SF_6] and [DIP] were well correlated as expected, although there was some evidence of tailing in [DIP] relative to [SF_6] as the ship moved away from the patch centre. A maximum [DIP] of 109 nmol/l was recorded on the first transect of the patch centre 7 h after release, in close agreement with the predicted average [DIP] of 124 nmol/l. The [DIP] maximum declined throughout both

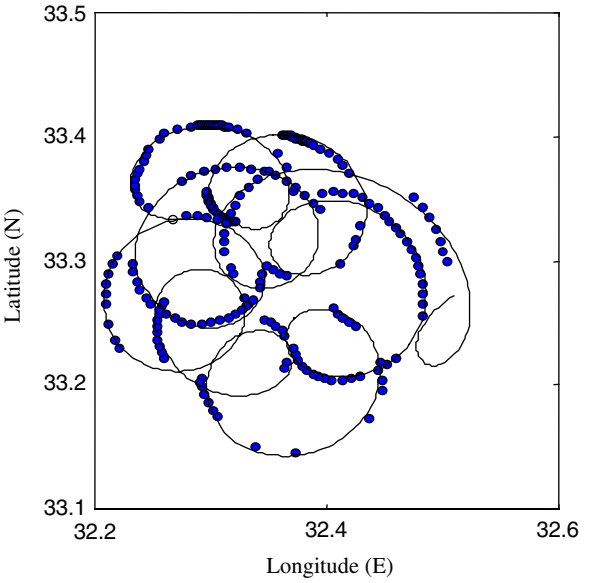

Fig. 2. Plot of drifter buoy movement during the 9-day experiment. The dots are positions obtained from the buoy, with the solid line a fit to the data constructed from an inertial oscillation with a period of 1.03 day, with the centre position, amplitude and phase of the oscillation varying at sub daily frequencies.

mapping sessions as a result of dilution and biological uptake of phosphate. Lagrangian SF_6 concentration maps generated at 2-day intervals indicate rapid expansion of the patch to an area of ~400 km^2 by day 8 (Fig. 4). Total patch SF_6 was estimated by objective analysis of the logged SF_6 data (Abraham et al., 2000), assuming a tracer layer depth of 16 m, with a least-squares fit to the trend in total SF_6 indicating an initial total at T0 of 0.32 mol SF_6 (Fig. 5). The discrepancy between the observed total and the estimated total SF_6 released suggests that either the initial mapping did not constrain the total area of the patch, or that losses to the atmosphere during the release and immediately after were significant. Lack of closure of the western patch boundary on day 1, as indicated by the error on the total SF_6 estimate (Figs. 4 and 5), suggests that limited mapping was the source of this discrepancy.

Wind-speed, as recorded by an onboard anemometer, was relatively low, averaging 5.0 ± 1.9 m/s (Fig. 6C), consistent with European centre for medium range weather forecasts (ECMWF) predicted wind-speed. Wind-speed was not recorded between days 4.5–7.5; during this period ECMWF

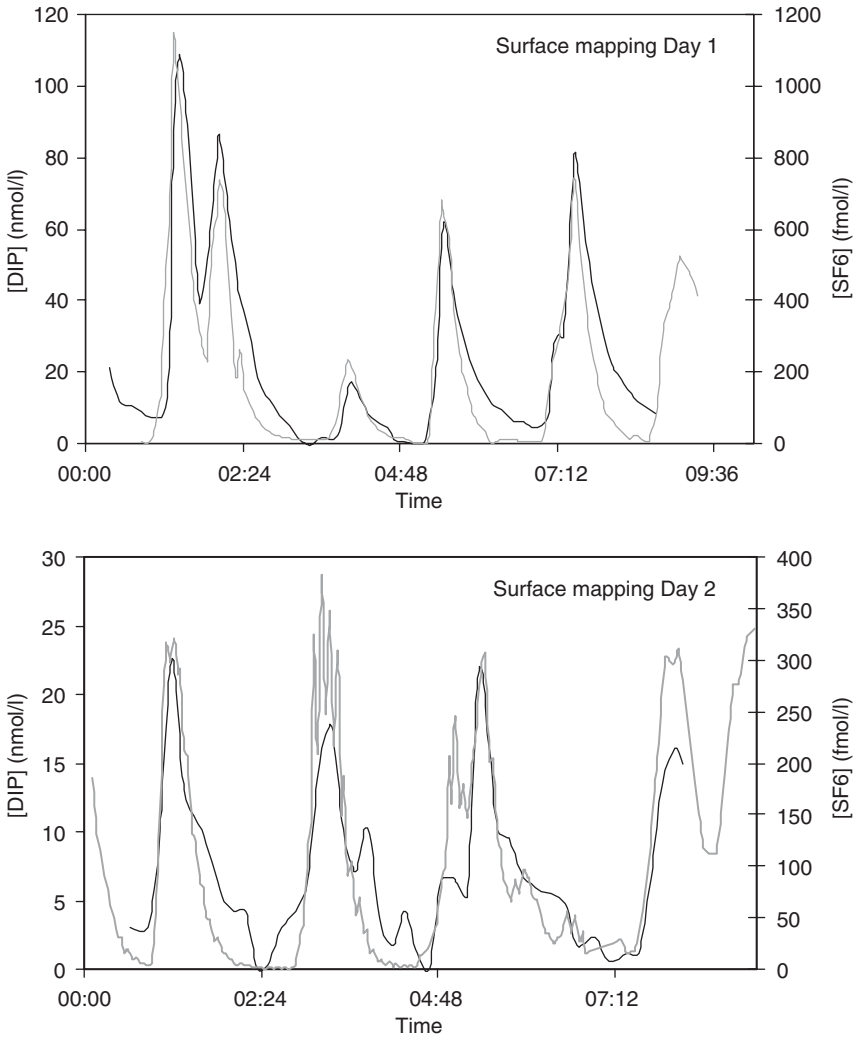

Fig. 3. Underway surface [DIP] (solid line) and [SF_6] (grey line) during surface mapping on days 1 and 2.

wind-speed confirmed that there was no significant increase (ECMWF experiment average 4.16 ± 1.6 m/s), although a maximum was observed on day 5.5. The transfer velocity was estimated from a wind-speed parameterisation (Nightingale et al., 2000), and applied to predict the decline in total SF_6 over the course of the experiment. The observed and expected data show similar trends with loss of ~50% of the SF_6 by day 8 (Fig. 5). Despite the low wind-speed the relatively shallow surface mixed layer of 16 m assisted loss to the atmosphere, resulting in similar ventilation loss rates to that reported for tracer releases in regions characterised by high wind-speeds but deeper surface mixed layers (Law et al., 2003).

3.2. Vertical evolution of the patch

The initial vertical profile on day 1 exhibited a distinct maximum in both [SF_6] and [DIP] at 20 m, deeper than the initial release depth of 9–11 m. Variability in SF_6 depth was apparent between 14 and 20 m over days 1–4, with an average mixed layer of ~16 m (Fig. 6A). [SF_6] at the patch centre was initially 1500 fmol/l (~1650 times background concentrations), but declined rapidly to a maximum of 51 fmol/l (~56 × background concentrations) on day 8 (Fig. 7). Potential density (σ_t) decreased in the mixed layer as the surface water warmed by ~1 °C during the 9-day experiment, with the warming reflected in a deepening of the isopycnals

within, and at the base of the mixed layer to day 5 (Fig. 6A). Generally SF_6 was retained above the $\sigma_t = 27.95$ isopycnal, although variability in the

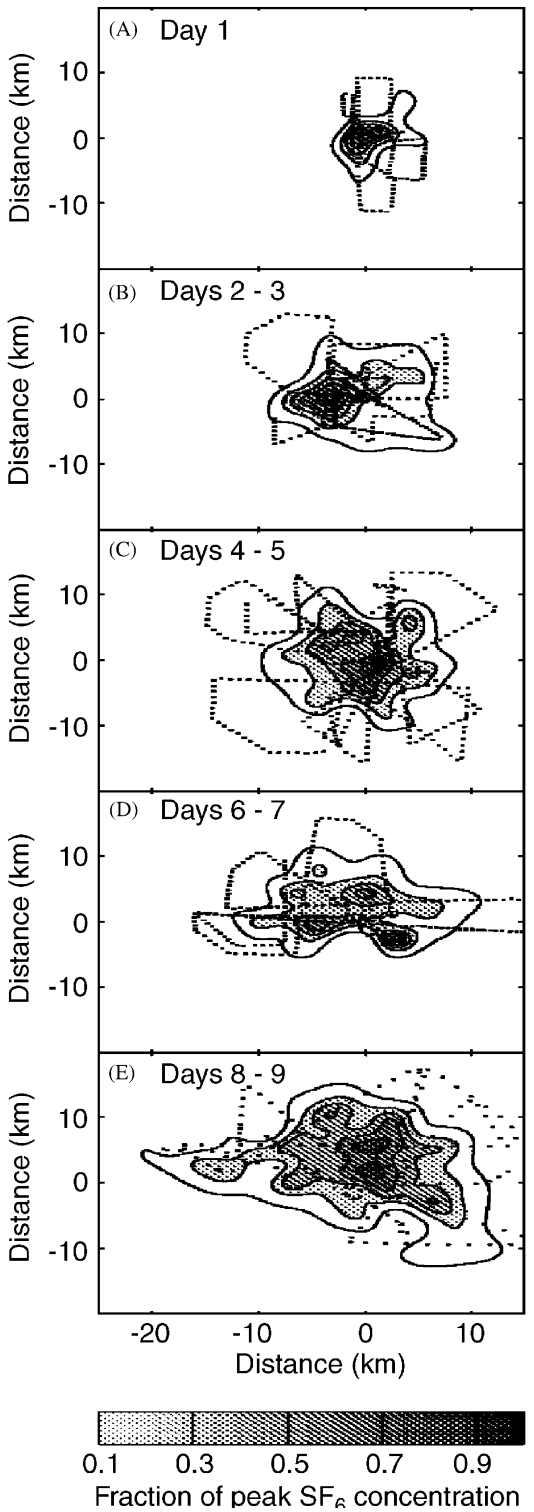

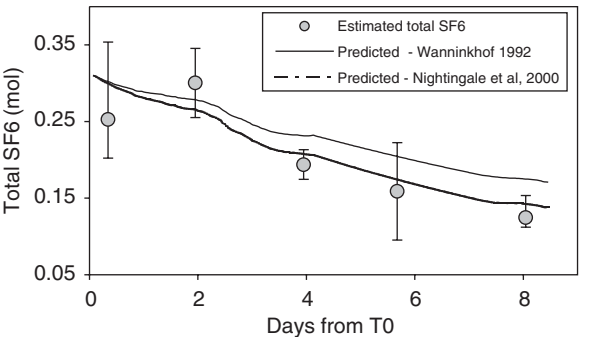

Fig. 5. Total observed SF_6, and two estimates of the predicted loss trend using the transfer velocity–wind-speed parameterisations of Wanninkhof (1992) and Nightingale et al. (2000), ECMWF-predicted wind-speeds and a mixed layer depth of 16 m. The error on the observed total SF_6 estimates was generated from the degree of patch boundary closure for each objective map.

SF_6–isopycnal relationship was apparent preventing the derivation of a vertical diffusion rate (K_z). Minor shallow structure in both SF_6 and density profiles on days 1–2 may reflect diel warming, although this was eroded by increased wind-speeds on days 3–4, as indicated by the buoyancy frequency, N^2 (Fig. 6B). On days 5–6 an increase in wind-speed to 8.2 m/s caused SF_6 to deepen to 25 m, coincident with deepening of the isopycnals and a marked decrease in stability at the base of the mixed layer as indicated by N^2. Fig. 6B shows that the enhanced vertical mixing during this period disrupted the seasonal pycnocline, pushing the N^2 maximum down to 30 m. It is uncertain whether subsequent stratification after this event resulted in isolation of SF_6 and phosphate below the seasonal pycnocline; although there is no evidence in the subsequent SF_6 profiles, elevated [DIP] was apparent between 20 and 40 m on day 6 (data not shown). In addition, examination of individual vertical profiles (Fig. 7) identified some degree of decoupling between tracer and nutrient, with phosphate

Fig. 4. Lagrangian contour plots of [SF_6] at 2-day intervals. The contours are based on an objective map to the logarithm of the [SF_6] data, and plotted as the fraction of the maximum [SF_6] in each 2-day interval, with the concentration assumed to fall to a background value of 1 fmol/l. A length-scale of 3 km was used to construct the map. Before mapping, the positions of the [SF_6] data were corrected for the drift of the buoy, using the fitted curve in Fig. 2, and corrected for a 15-min lag between sampling and recorded analysis time. No correction is included for rotation.

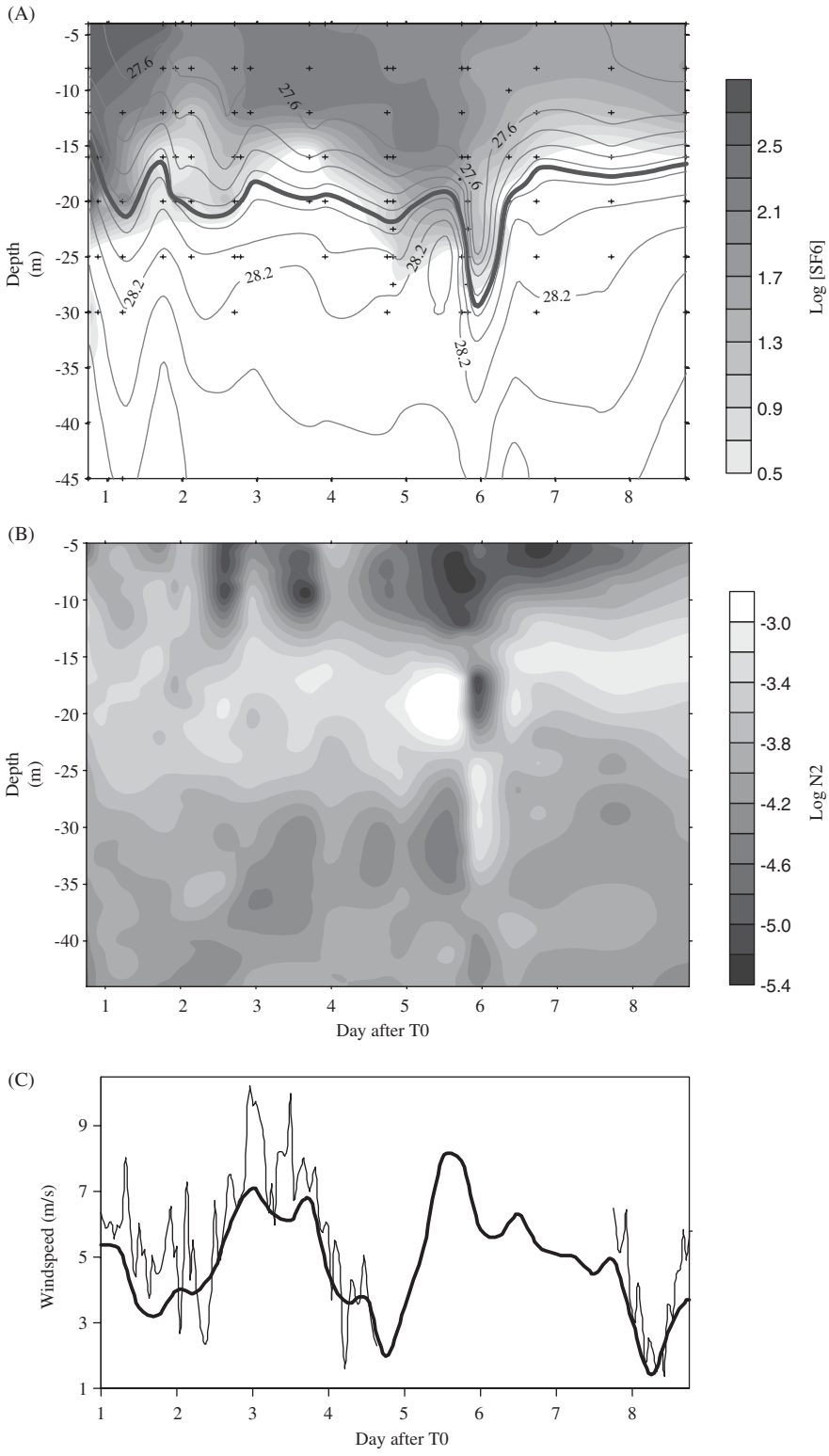

Fig. 6. Contour depth plots of (A) log [SF_6] (colour bar) with sample depths indicated (crosses), and overlain by σ_t contour lines (depth resolution 1 m at all stations) with the 27.95 isopycnal indicated in bold, and (B) log N^2 (depth resolution 1 m at all stations). (C) Windspeed measured during the experiment (thin line) and predicted from ECMWF (thick line).

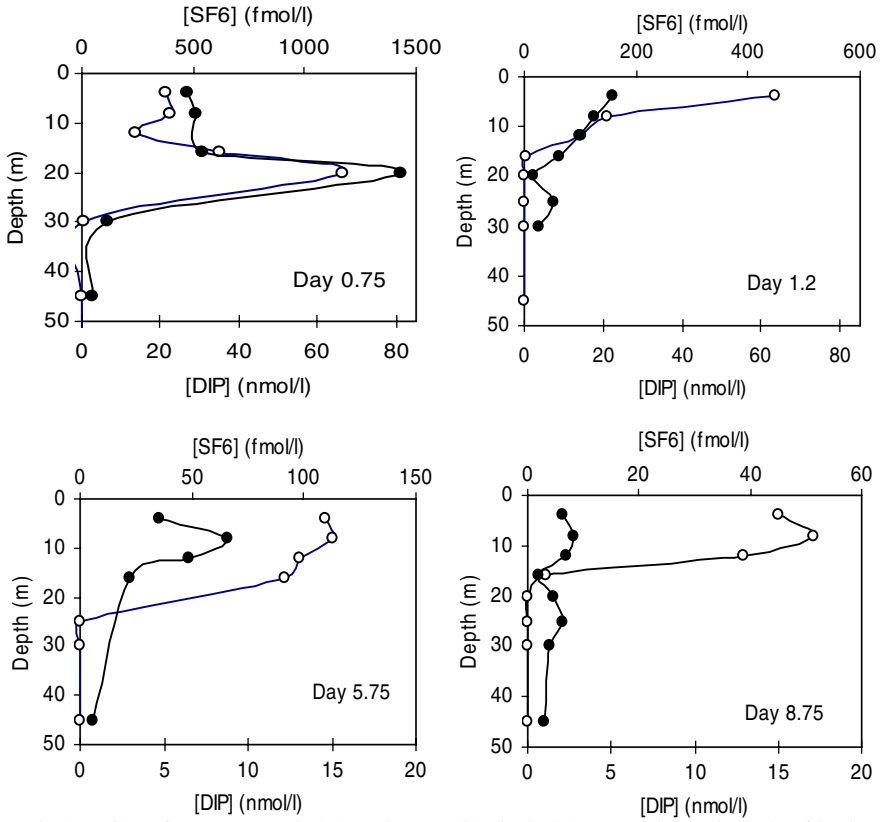

Fig. 7. Vertical profiles of $[SF_6]$ (open circles) and [DIP] (black circles). Note change in scale of both parameters.

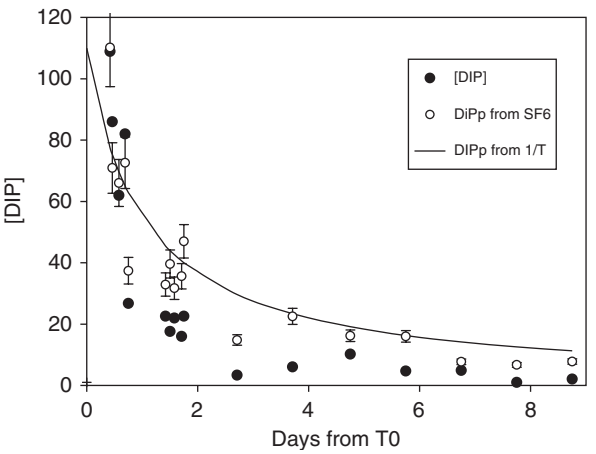

Fig. 8. [DIP] and DIPp for all surface samples, where DIPp was obtained by correcting $[SF_6]$ for air–sea exchange and multiplying by the molar ratio of 92000 ($[SF_6]$:[DIP]). The error on DIPp is 11.6%, based upon the observed variation in $[SF_6]$:[DIP] during the initial mapping. The solid line is a fit of $1/T$, where T is time after the release, obtained from a best fit to the DIPp data.

apparent below the seasonal pycnocline at 16 m without excess SF_6 on days 1.2, and at the end of the experiment on day 8.75, possibly due to phosphate release during remineralisation of vertically exported particulate material.

3.3. Predicted phosphate concentration

[DIP] decreased rapidly at the patch centre, falling to 25% of the initial concentration by day 3 (Fig. 8). The general coherence and correlation between $[SF_6]$ and [DIP] (Fig. 3) confirmed that $[SF_6]$ was an effective empirical proxy for [DIP], and could be applied to discriminate between conservative dilution losses and biological uptake of phosphate. Assuming that lateral dilution loss was the only process influencing [DIP] at the patch centre, then the predicted mixed layer phosphate concentration (DIPp), can be calculated from $[SF_6]$ using the initial [DIP]:$[SF_6]$ ratio of 92 000 ($\pm$10 672) observed during mapping on day 1. DIPp estimates were obtained using the $[SF_6]$ maximum recorded on each transect of the patch during surface mapping on day 2 (Fig. 3), and also $[SF_6]$ measurements to a depth of 12 m at all IN stations (Figs. 6 and 7). On day 1 DIPp was calculated from $[SF_6]$ to a depth of 16 m to

accommodate the deeper maximum on this cast (Fig. 7). This calculation required each [SF_6] to first be corrected for cumulative ventilation loss since T0, using wind-speed data (ECMFW) a transfer velocity wind-speed parameterisation (Nightingale et al., 2000), and a mixed layer depth of 12 m. Only the [SF_6] maximum at the patch centre was used to calculate DIPp, and we assume that the [SF_6] maxima obtained during mapping on days 1 and 2 were representative of the patch centre. DIPp in surface samples showed a rapid decline of 70% by day 3 and 93% by day 8 (Fig. 8). An alternative estimate of DIPp assuming dilution of the patch at the rate $1/T$, where T is time after release, showed good agreement with the trend in [SF_6]-derived DIPp, although there was deviation on days 1 and 2 (Fig. 8). The [SF_6]-derived DIPp was used in subsequent analysis as it accounted for dilution of the actual water sample as opposed to an idealised dilution for the patch centre. Prediction of DIPp from $1/T$ would not account for variation in the position of the IN station relative to the patch centre, and would also be influenced by the selected [DIP] value at T0.

4. Discussion

4.1. The impact of dilution on the biological response to the phosphate addition

Mixing in the surface ocean is a critical determinant of the scale, magnitude and longevity of a phytoplankton bloom (Martin, 2003). This is particularly true for in situ fertilisation experiments in which the initial release is constantly diluted with unperturbed water from outside the patch (Abraham et al., 2000). The initially rapid dilution of the CYCLOPS patch may have impacted both the overall biological response to the P addition, and its manifestation, by reducing the accumulation of phytoplankton and bacterial biomass at the IN station. A trend of decreasing chlorophyll (Psarra et al., 2005), and rapid increase in heterotrophic biomass inside the patch were reported for CYCLOPS (Pitta et al., 2005; Pasternak et al., 2005), in marked contrast to previous microcosm experiments using E. Mediterranean waters which have shown increases in phytoplankton productivity (Zohary and Robarts, 1998). The CYCLOPS results also contrast with in situ iron experiments in HNLC regions in which the picophytoplankton exhibited transient increases in abundance, and the larger phytoplankton significant biomass increase (Boyd et al., 2000). The results from CYCLOPS provisionally suggest that the bacteria out-competed the phytoplankton for the added phosphate (Flaten et al., 2005; Psarra et al., 2005). Heterotrophic bacteria are typically smaller than phytoplankton with a surface area:volume ratio that provides a competitive physiological advantage in sequestering dissolved nutrients. In addition, the heterotrophic bacteria had the additional advantages of dominating the pre-release microbial community (Pitta et al., 2005), and could access DOC and DON to support a heterotrophic bacterial response to the added P (Krom et al., 2005). However despite the observed increase in bacterial production rate at the patch centre (Pitta et al., 2005), there was no corresponding increase in bacterial biomass, suggesting either efficient top-down control by grazers or amelioration of biomass accumulation by dilution.

To examine whether dilution was responsible, the lateral diffusion rate, K_y, was estimated by fitting Gaussians to the patch centre for each SF_6 map and calculating the increase in area (s^2) with time from $s^2 = 2K_y t$. Expansion of the patch was uniform with time (Fig. 9A), with a lateral diffusion rate of $23 \pm 2\,m^2\,s^{-1}$, in agreement with estimates from previous tracer releases in the Equatorial Pacific ($25 \pm 5\,m^2\,s^{-1}$; Abraham et al., 2000; Stanton et al., 1998) and N.E. Atlantic ($22 \pm 10\,m^2\,s^{-1}$; Martin et al., 2001). This observed K_y reflects control of mixing at the mesoscale, with higher rates recorded in eddies, such as in CYCLOPS, where current strain is low and lateral evolution is primarily controlled by diffusive mixing. Conversely, current strain increases at distance from an eddy centre and the resulting filamentation of a patch limits diffusion, as observed in the southern Ocean (Abraham et al., 2000). The dilution rate, estimated from the relative rate of increase in the patch area, $(d\sigma^2/dt)/\sigma^2 = 2K_y/\sigma^2$, was initially close to 1 day^{-1} but declined rapidly as the patch size increased (Fig. 9B).

The conservative loss of a biogeochemical tracer, such as chlorophyll or phosphate, is then a function of dilution rate and the concentration gradient between IN and OUT patch water. For an exponentially growing biological population, the KISS model (Skellam, 1951; Kierstead and Slobodkin, 1953) suggests that a population at the patch centre will only increase in biomass if its growth rate exceeds the dilution rate. No difference was

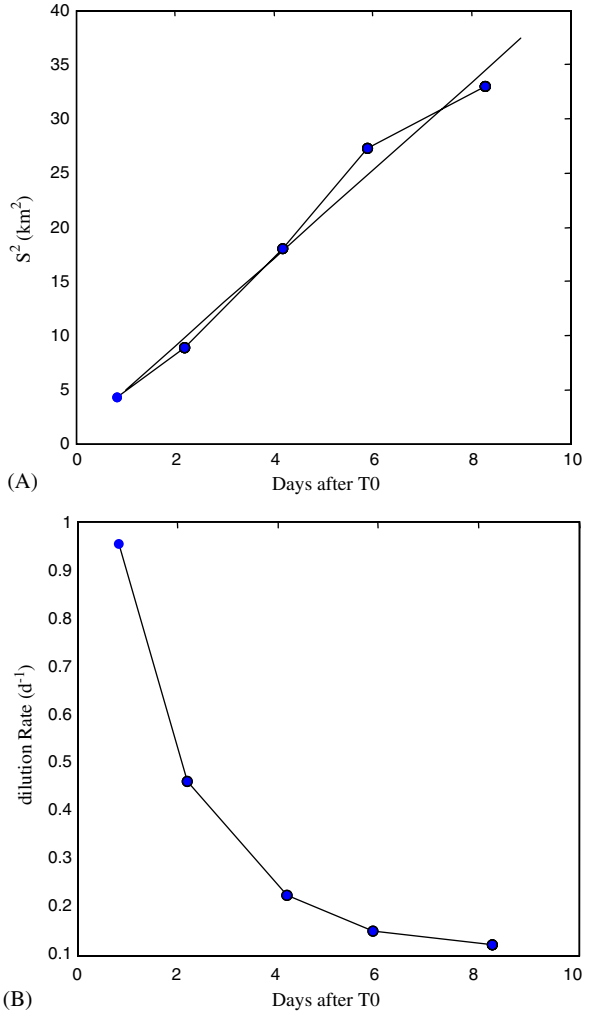

Fig. 9. (A) Increase in s^2 for the patch centre in km^2. (B) Decrease in the critical growth rate, or dilution rate, as a function of days after the P addition.

observed in phytoplankton growth rate between IN and OUT stations during CYCLOPS (Psarra et al., 2005), and so patch dilution would have had little effect on phytoplankton abundance at the patch centre. Conversely, bacterial net growth rates were $\sim$2 day^{-1} inside the patch and $\sim$1 day^{-1} at the OUT stations. An analysis of the effect of diffusion on the bacterial abundance within the patch is presented in Appendix A. The analysis predicts, not surprisingly, that the increase in bacterial abundance at the patch centre would be greatest at zero diffusion and decline with increasing diffusion (Fig. 10). However, the impact of increasing diffusion is less significant than might be expected as bacterial abundance outside the patch was not zero and so there is lateral supply of bacteria to the patch centre. Consequently, the predicted difference in bacterial abundance at the patch centre at a low K_y ($4\,m^2\,s^{-1}$; Abraham et al., 2000), and high K_y ($23\pm2\,m^2\,s^{-1}$, CYCLOPS) will be $<15\%$, assuming all other terms are equal.

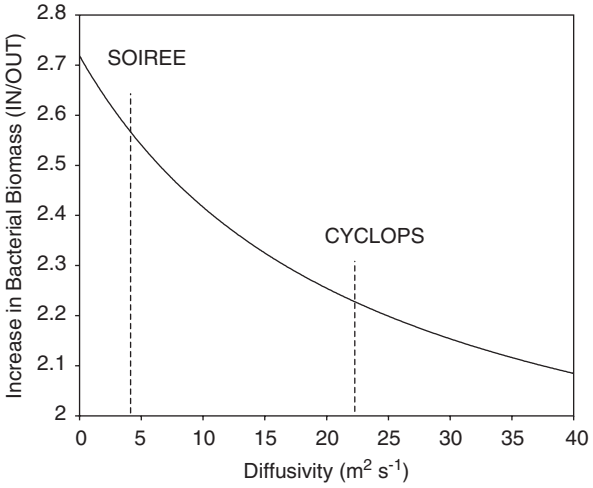

Fig. 10. The predicted bacterial biomass increase on day 1, expressed as a ratio (IN/OUT), against lateral diffusion rate, estimated using a differential ($\alpha-\alpha_0$) bacterial growth rate of 1 day^{-1} (see Appendix A). Biomass accumulation at a lower diffusivity of $4\,m^2\,s^{-1}$ recorded during SOIREE (Abraham et al., 2000) is indicated for comparison at a low diffusivity.

The analysis demonstrates that a bacterial growth rate of 2 day^{-1} at the patch centre should have produced an increase in bacterial abundance on day 1, regardless of diffusion rate, and predicts that IN station bacterial abundance would have exceeded that of the OUT station by a factor of $\sim$2.25 (Fig. 10). The discrepancy between the predicted increase and the observed lack of change in bacterial biomass (Pitta et al., 2005) indicates a non-conservative bacterial loss term of $\sim$0.83 day^{-1}. Viral abundance data (W. Wilson, pers. comm.) suggests that viral lysis was unlikely to be a significant factor, and so grazing was most likely responsible for the lack of increase in bacterial abundance. The biomass of the heterotrophic nanoflagellates did increase at the patch centre until day 2, and the ciliates increased significantly on day 1 (Pitta et al., 2005), despite also being subject to dilution. It appears that a rapid response in the food chain transferred the observed increase in bacterial production, and possibly heterotrophic nanoflagellate production, into ciliate biomass. An alternative hypothesis that the change in food quality (e.g. increase in P content), rather than quantity (biomass), was responsible for the

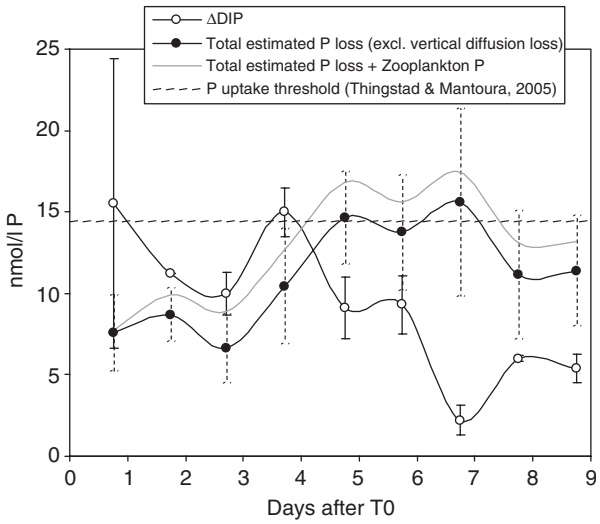

Fig. 11. Temporal trend in ΔDIP and total biological P uptake (Part-P accumulation + Part-P loss to dilution). The mean ΔDIP is shown for samples in the surface 12 m at all IN stations. The error bars (dashed) on the total biological P uptake estimates are based on the error for Part-P measurements (Flaten et al., 2005) applied to both Part-P accumulation at the patch centre, and lateral Part-P loss to dilution. The dashed horizontal line indicates the predicted threshold for biological P uptake before the system shifts into nitrogen limitation (Thingstad and Mantoura, 2005).

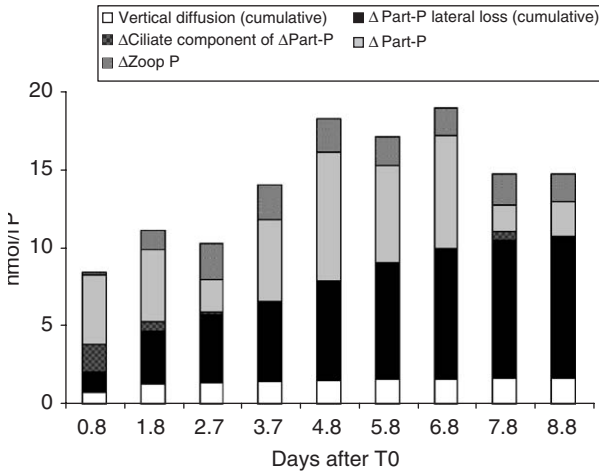

Fig. 12. Temporal trend in P loss processes at the patch centre. Cumulative vertical diffusion loss was calculated from the mid-point DIP gradient across the seasonal pycnocline between each sample, using a K_z of $1 \times 10^5\,m^{-2}\,s^{-1}$ (Law et al., 2003); ΔPart-P was the particulate P at each IN station minus OUT station Part-P (Flaten et al., 2005); cumulative ΔPart-P lateral loss was calculated from the IN/OUT gradient in ΔPart-P and dilution rate; the Δciliate component of ΔPart-P was estimated by subtracting OUT station ciliate carbon biomass (Pitta et al., 2005) from each respective IN ciliate carbon biomass and applying a C:P ratio of 250 (Flaten et al., 2005); and Δzoop was the maximum P incorporated into mesozooplankton estimated by subtracting OUT station mesozooplankton carbon biomass from each IN station mesozooplankton carbon biomass estimate (Pasternak et al., 2005), and applying a C:P ratio of 250.

observed doubling in ciliate abundance, is discussed elsewhere (Flaten et al., 2005; Thingstad, 2005; Thingstad et al., 2005). Regardless, the analysis suggests that dilution of the patch would not have significantly restricted accumulation of bacterial biomass, and that consequently heterotroph grazing was most likely responsible.

4.2. A phosphate budget incorporating physical and biological loss terms

The dilution rate was also used to generate a budget and partition loss of the added phosphate, as with a previous application in an in situ iron experiment (Bowie et al., 2001). Phosphate dynamics at the patch centre during CYCLOPS were dominated by dilution, with two-thirds of the phosphate transferred laterally from the patch centre within 48 h (Fig. 8). If [DIP] was solely determined by dilution with water of effectively zero concentration, then there would be little difference between [DIP] and DIPp. However divergence between these two parameters was apparent between days 1 and 4, before convergence towards the end of the experiment (Fig. 8). The deficit, ΔDIP = DIPp–[DIP], then represents the non-conservative biological removal of phosphate from the dissolved inorganic form and vertical transport from the surface mixed layer at the patch centre. ΔDIP increased to 15.5 ± 8.9 nmol/l during day 1 (Fig. 11), with the large error on this estimate arising from variability in $[SF_6]$ to 20 m. ΔDIP subsequently decreased on day 2 but increased again to 15 ± 1.5 nmol/l by day 4, when it was equivalent to ~43% of the DIPp. By day 7 ΔDIP had declined to ~2 nmol/l, but rose again to 5 nmol/l on days 8–9.

The individual processes contributing to phosphate loss can be constrained within a simple budget. Vertical diffusion across the seasonal pycncocline was a sink for phosphate, but was not determined directly. Instead the vertical diffusivity (K_z) at the base of the mixed layer was estimated from N^2, using the relationship observed in previous tracer experiments (Law et al., 2003) to obtain a K_z estimate of 1×10^{-5} $(2.5 \times 10^{-6}$–$8 \times 10^{-5})\,m^2\,s^{-1}$.

Phosphate loss at the patch centre via vertical diffusion was most significant on day 1 when the [DIP] gradient across the seasonal pycnocline was greatest, with a diffusive flux of 0.19 (0.05–1.5) nmol $m^{-2} s^{-1}$ and corresponding decrease in [DIP] of 0.77 (0.2–6.1) nmol/l. The vertical flux would have subsequently declined as lateral dilution reduced the vertical gradient across the seasonal pycnocline. Vertical loss of phosphate was irreversible and accounted for a cumulative loss of 1.7 (0.4–13.5) nmol/l over the 9-day experiment (Fig. 12). It should be noted that vertical diffusive loss of phosphate would be conservative, and so would not contribute to ΔDIP. Similarly vertical loss of DIP associated with increased vertical diffusion or advection during the period of increased winds on days 5–6 will also be conservative and would not influence the ΔDIP estimate. Another potential abiotic sink for phosphate is adsorption onto iron oxyhydroxides in dust particles with subsequent vertical export (Krom et al., 1991). However, dust addition to an onboard microcosm experiment during CYCLOPS resulted in an increase in [DIP] (Herut et al., 2005), and, as there was no significant aeolian deposition during the experiment (Carbo et al., 2005), this was not considered in the phosphate budget. Transformation into the organic phase is also a possibility, as dissolved organic phosphorus represents the largest pool of dissolved P in the surface waters of the Cyprus Eddy (Krom et al., 2005). IN station DOP data showed some variability during the first 3–4 days of CYCLOPS but no clear trends, and so the dissolved organic pool was not considered to be a significant sink for the added phosphate. It appears then that biological processes represented the major sink for phosphate, and so the primary component of ΔDIP. The rapid initial increase in orthophosphate turnover time on day 1 coincided with an increase in particulate phosphorous (Part-P) from 8.5 (±1.25) to 15 (±1.9) nmol/l at the patch centre, which remained elevated until day 7 (Flaten et al., 2005). This net increase of ~6.5 nmol/l (ΔPart-P) was equivalent to ~50% of the maximum ΔDIP, indicating transfer of P to another pool or transport from the patch centre. Lateral loss of Part-P from the patch centre was calculated using the Part-P IN–OUT gradient and assuming dilution at the rate $1/T$, and accounted for 2.1 nmol/l/day on day 2, declining to 0.23 nmol/l/day by day 9 (Fig. 12). Approximately 50% of the Part-P was laterally exported at 3 days after release, with a total of 9.1 (6.5–11.8) nmol/l lost from the patch centre by the end of the experiment.

It is difficult to constrain the transfer of Part-P through the microbial food web. Despite the increase observed in bacterial production (Pitta et al., 2005) there was no corresponding increase in bacterial biomass, and phytoplankton abundance declined, at least during the initial phase of the experiment (Psarra et al., 2005). However, significant accumulation of biomass in the microzoograzers suggests a rapid increase in bacterivory within the first 24 h (Pitta et al., 2005). These organisms can rapidly respond to increases in prey abundance with a growth rate similar to that of their prey (Thingstad and Rassoulzadegan, 1995). Shipboard microcosm incubations during CYCLOPS indicated that bacterivory was most significant on days 1–3 (T. Tanaka, pers. comm.), and coincided with an increase in heterotrophic ciliate biomass at the patch centre (Pitta et al., 2005). The ciliate component of Part-P was estimated (Fig. 12), using a C:P ratio of 250 characteristic of the cyanobacterium *Synnecochoccus* which dominated the autotrophic component during CYCLOPS (Flaten et al., 2005). As the heterotrophic ciliate biomass may have derived from bacteria with a C:P ratio as low as 50, the estimate in Fig. 12 is probably a conservative estimate of the ciliate biomass component of the Part-P.

Observations suggest that the phosphate was rapidly channelled through the microzooplankton to the mesozooplankton from day 2 (Thingstad et al., 2005). Mesozooplankton carbon biomass increased on day 3, coincident with the decline in the ciliate biomass, and remained elevated to the end of the experiment (Pasternak et al., 2005). Further supporting evidence was provided with increases in faecal pellets and maxima in egg production and mesozooplankton gut fullness on day 4–5 (Pasternak et al., 2005). Egg production by mesozooplankton and food availability are tightly linked (Hirche, 1996), suggesting that the observed increase was directly linked to increased prey abundance or quality (Flaten et al., 2005). However, the actual loss of P due to faecal pellet and egg production was negligible in terms of ΔDIP. It is also impossible to differentiate between the increase in mesozooplankton biomass that arose from active lateral migration into the patch centre, and that which derived from growth of the extant mesozooplankton population. If we assume that the increase in mesozooplankton biomass, of 0.105 g C m^{-2} on

day 3 (Pasternak et al., 2005), was entirely due to growth of the extant mesozooplankton population in the upper 125 m, then application of the C:P ratio of 250 suggests that only 2.1 nmol/l P would have been incorporated into mesozooplankton biomass in the patch (Fig. 12). However, this would require rapid maturation of a extant cohort of copepodites, which was not apparent in the pre-release surveys (Pasternak et al., 2005). Consequently the estimated P loss as mesozooplankton biomass should be considered as an upper limit, as it is likely that a proportion of the observed mesozooplankton migrated laterally into the patch in response to increased prey abundance.

The total cumulative biological P uptake, estimated by summing ΔPart-P and the cumulative ΔPart-P loss to dilution (Fig. 12), was 14.7 ± 2.8 nmol/l by day 4.7 and reached a maximum of 15.6 ± 5.6 nmol/l by day 6.7 (Fig. 11). This is in excellent agreement with the ΔDIP estimate (15 ± 1.5 nmol/l), and two other independent estimates of biological P uptake in the surface waters of the Cyprus Eddy. Microcosm experiments using water collected from the CYCLOPS phosphate pilot experiment in 2001 identified that 10–25 nmol/l phosphate could be utilised by the biota before another mechanism prevented further P uptake (Flaten et al., 2005). This observation was further refined by alkaline phosphatase measurements during CYCLOPS (Thingstad and Mantoura, 2005), that identified a biological P uptake threshold of $\sim 14.4 (\pm 3.75)$ nmol/l (Fig. 11), above which the ecosystem is driven into nitrogen limitation. Subtraction of the mean biological P uptake from the reported P uptake threshold (Thingstad and Mantoura, 2005) leaves a residual of 1.4 nmol/l P, which is within the analytical error for [DIP]. As the non-conservative phosphate loss, ΔDIP, was fully accounted for by the particulate phase, this indicates that remaining sinks for phosphate were insignificant in terms of the budget. Consequently, although the phosphate addition stimulated an increase in mesozooplankton biomass, the actual transfer of P into mesozooplankton biomass appears to have been insignificant. The degree of closure in this budget is surprising, bearing in mind that the vertical export of particles and trophic transfer of P to secondary consumers are not considered. The appearance of phosphate below the seasonal pycnocline towards the end of the experiment was possibly attributable to remineralisation, as indicated by ammonium and nitrite increases at depth (Krom et al., 2005), and the increase in faecal pellets to 125 m depth (Pasternak et al., 2005). Although these loss terms are not considered in the budget, neither is the potential N supply from excretion by mesozooplankton migrating laterally into the patch, and the lateral supply of N from outside the patch. Results from the microcosm and alkaline phosphatase experiments indicate that $\sim 230 \pm 60$ nmol/l N was available by the biota to sustain the uptake of 14.4 nmol/l phosphate (Thingstad and Mantoura, 2005). The resulting gradient between the IN and OUT stations would have maintained lateral supply of dissolved nitrogen to the patch centre, with the result that biological P uptake would have exceeded the 14.4 nmol/l threshold observed in the microcosm experiments.

As is apparent from the above analysis, mixing and dilution with unperturbed water would not have altered the response to the P addition, but did influence both magnitude and manifestation. During the initial days of the experiment, dilution resulted in a decrease in bacterial abundance at the patch centre but this was exceeded by another loss term that was most likely grazing pressure. However, with the lateral loss of $>60\%$ of the added phosphate by day 2 and $>50\%$ of the Part-P produced by day 3 dilution clearly impacted the observed response. This has implications for the location of mesoscale fertilisation experiments, in that the advantages of low shear and limited advection of a patch at the centre of an eddy, may be overshadowed by the reduced biological response that results at elevated dilution.

Acknowledgements

We thank Tassos Tselepides, Michael Krom and Pre Carbo for the successful coordination of this experiment and the CYCLOPS programme. We also thank George Zodiatis and Panos Drakopoulos for CTD operation and data assimilation, Andy Rees for assistance with nutrient analysis, and the officers and crew of the R/V *Aegaeo* for their assistance. Paul Wassman and Phil Boyd provided useful advice and comments. Data from the European centre for medium range weather forecasts (ECMWF) operational analysis were supplied by the British Atmospheric Data Centre (BADC) with access and manipulation by Tim Smyth. The SeaWiFS image was processed at the Plymouth Marine Laboratory by the Remote Sensing group, with the SeaWiFS data courtesy of NASA and

Orbimage Inc. Thanks also to the University of East Anglia for the loan of the release pumping system and Hydrosphere UK Ltd. for the loan of the drifter buoy housing. This work was funded as part of the EC Framework V CYCLOPS Project (EKV3-CT-1999-00009).

Appendix A

In determining the effect of mixing on an isolated patch with a perturbed growth rate during the first day following P addition, it is assumed that the dynamics within the patch may be captured by the following assumptions. We assume that growth and loss terms are in balance outside the patch and that the concentration is steady; that within the patch growth is enhanced by phosphate addition but the per capita mortality remains the same as outside; that there is diffusive mixing between the patch and the surrounding water; and that as water and plankton are mixed into the patch, the growth rate of the plankton adjusts rapidly to the increased nutrient so that mixing influences the concentration but not the intrinsic growth rate.

Subject to these assumptions, the growth at the patch centre can be expressed through the following simple equation

$$\frac{\partial C}{\partial t} = \alpha C - \alpha_0 C + k\frac{\partial^2 C}{\partial x^2}, \tag{A1}$$

where C is the density of the population, α is the growth rate within the patch and α_0 is the growth rate outside the patch. The growth rate outside the patch is included as we assume that this is equal to the mortality.

If the patch is a Gaussian, then at the patch centre the mixing term is

$$k\frac{\mathrm{d}^2 C}{\mathrm{d}x^2} = -2k(C - C_0)/\sigma^2, \tag{A2}$$

where σ is the standard deviation of the patch. While the patch is dispersing, the size of the patch increases linearly with time

$$\sigma^2 = 2k(t + t_0), \tag{A3}$$

where the constant t_0 is determined from the initial patch size, σ_0, as $t_0 = \sigma_0^2/2k$. By inserting this into Eq. (A1) the change in concentration at the patch centre can be written as

$$\frac{\partial C}{\partial t} = (\alpha - \alpha_0)C - \frac{C - C_0}{t + t_0}. \tag{A4}$$

Eq. (A3) can be solved to estimate the effect of dispersal on the growth of the patch. If $\alpha - \alpha_0 > 1/(t + t_0)$ then there will be a net positive increase in the concentration C, which is equivalent to the KISS condition (Skellam, 1951; Kierstead and Slobodkin, 1953). Otherwise, the concentration will increase if and only if

$$C < \frac{C_0}{1 - (\alpha - \alpha_0)(t + t_0)}. \tag{A5}$$

Eq. (A3) can be solved fully by first converting to dimensionless variables. If we define $C^* = C/C_0$, $t^* = (\alpha - \alpha_0)t, t_0^* = (\alpha - \alpha_0)t_0$, then the equation becomes

$$\frac{\partial C^*}{\partial t^*} = C^* - \frac{C^* - 1}{t^* + t_0^*}. \tag{A6}$$

This has the solution

$$C^*(t^*) = \frac{(1 + t_0^*)\,\mathrm{e}^{t^*} - 1}{t^* + t_0^*}, \tag{A7}$$

where the initial condition is $C^*(0) = 1$. If the diffusivity is small, then t_0^* will be large, and the solution is simply exponential growth, $C^*(t^*) = \mathrm{e}^{t^*}$. If the diffusivity is large, on the other hand, then $t_0^* = 0$, and the equation reduces to $C^*(t^*) = (\mathrm{e}^{t^*} - 1)/t^*$. When $t^* = 1$, as in Fig. 10, then the concentration at the patch centre is $C^* = \mathrm{e} - 1/(1 + t_0^*)$. In terms of the dimensional variables this can be written as

$$C/C_0|_{t=1/(\alpha-\alpha_0)} = \mathrm{e} - 1/(1 + (\alpha - \alpha_0)\sigma_0^2/2k).$$

This function is shown in Fig. 10, with the concentration at the patch centre decreasing when diffusivity increases, as expected.

References

Abraham, E.R., Law, C.S., Boyd, P.W., Lavender, S.J., Maldonado, M.T., Bowie, A.R., 2000. Importance of stirring in the development of an iron-fertilized phytoplankton bloom. Nature 407, 727–730.

Banse, K., 1991. Iron availability, nitrate uptake, and exportable new production in the Subarctic Pacific. Journal of Geophysical Research 96 (C1), 741–748.

Bonin, D.J., Bonin, M.C., Berman, T., 1989. Mise en evidence experimentale des facteurs nutritifs limitants de la production du micro-nanoplancton et de l'ultraplancton dans une eau cotiere de la Mediterranee orientale (Haifa Israel). Aquatic Sciences 51, 129–159.

Bowie, A.R., Maldonado, M.T., Frew, R.D., Croot, P.L., Achterberg, E.P., Mantoura, R.F.C., Worsfold, P.J., Law,

C.S., Boyd, P.W., 2001. The fate of added iron during a mesoscale fertilisation experiment in the Southern Ocean. Deep-Sea Research II 48 (11–12), 2703–2743.

Boyd, P.W., Watson, A.J., Law, C.S., Abraham, E.R., Trull, T., Murdoch, R., Bakker, D.C.E., Bowie, A.R., Buesseler, K.O., Chang, H., Charette, M., Croot, P., Downing, K., Zeldis, J., et al., 2000. A mesoscale phytoplankton bloom in the polar Southern Ocean stimulated by iron fertilization. Nature 407, 695–702.

Boyd, P.W., Law, C.S., Wong, C.S., Nojiri, Y., Tsuda, A., Levasseur, M., Takeda, S., Rivkin, R., Harrison, P.J., Strzepek, R., Gower, J., McKay, R.M., Abraham, E., Arychuk, M., Barwell-Clarke, J., Crawford, W., Crawford, D., Hale, M., Johnson, K., Kiyosawa, J., Kudo, I., Marchetti, A., Miller, W., Needoba, J., Nishioka, J., Ogawa, J., Page, J.T., Robert, M., Saito, H., Sastri, A., Sherry, N., Soutar, T., Sutherland, N., Taira, Y., Whitney, F., Wong, S.-K.E., 2004. The decline and fate of an iron-induced subarctic phytoplankton bloom. Nature 428, 549–553.

Carbo, P., Krom, M.D., Homoky, W.B., Herut, B., 2005. Impact of atmospheric deposition on N and P geochemistry in the southeastern Levantine basin. Deep Sea Research II, this volume [doi:10.1016/j.dsr2.2005.08.014].

Christaki, U., Van Wambeke, F., Dolan, J.R., 2001. Nanoflagellates (mixotrophs, heterotrophs and autotrophs) in the oligotrophic Eastern Mediterranean: standing stocks, bacterivory and relationships with bacterial production. Marine Ecology Progress Series 181, 297–307.

Flaten, G.A., Skjoldal, E.F., Krom, M.D., Law, C.S., Mantoura, R.F.C., Pitta, P., Psarra, S., Tanaka, T., Tselepides, A., Woodward, E.M.S., Zohary, T., Thingstad, T.F., 2005. Studies of the microbial P-cycle during a Lagrangian phosphate-addition experiment in the Eastern Mediterranean. Deep Sea Research II, this volume [doi:10.1016/j.dsr2.2005.08.010].

Gruber, N., Sarmiento, J.L., 1997. Global patterns of marine nitrogen fixation and denitrification. Global Biogeochemical Cycles 11 (2), 235–266.

Hall, J.A., Safi, K., 2001. The impact of in situ Fe fertilisation on the microbial food web in the Southern Ocean. Deep-Sea Research II 48 (11–12), 2591–2613.

Herut, B., Krom, M.D., Pan, G., Mortimer, R., 1999. Atmospheric input of nitrogen and phosphorus to the Southeast Mediterranean: sources, fluxes, and possible impact. Limnology and Oceanography 44, 1683–1692.

Herut, B., Zohary, T., Krom, M.D., Mantoura, R.F.C., Pitta, P., Psarra, S., Rassoulzadegan, F., Tanaka, T., Thingstad, F., 2005. Trophic tunneling by dust: biochemical response of East Mediterranean surface water to Sahara dust addition, onboard microcosm experiment and field observations. Deep Sea Research II, this volume [doi:10.1016/j.dsr2.2005.09.003].

Hirche, H.-J., 1996. The reproductive biology of the marine copepod, *Calanus finmarchicus*—a review. Ophelia 44, 111–128.

Kierstead, H., Slobodkin, L.B., 1953. The size of water masses containing plankton blooms. Journal of Marine Research 12, 141–147.

Klein, B., Roether, W., Manca, B., Bregant, D., Beitzel, V., Kovacevic, V., Luchetta, A., 1999. The large deep water transient in the Eastern Mediterranean. Deep Sea Research I 46, 371–414.

Krom, M.D., Kress, N., Brenner, S., Gordon, L.I., 1991. Phosphorus limitation of primary productivity in the eastern Mediterranean. Limnology and Oceanography 36, 424–432.

Krom, M.D., Brenner, S., Kress, N., Neori, A., Gordon, L.I., 1992. Nutrient dynamics and new production in a warm-core eddy from the E. Mediterranean. Deep-Sea Research II 39, 467–480.

Krom, M.D., Groom, S., Zohary, T., 2003. The Eastern Mediterranean. Blackwell, Oxford.

Krom, M.D., Woodward, E.M.S., Herut, B., Kress, N., Carbo, P., Mantoura, R.F.C., Spyres, G., Thingsted, T.F., Wassmann, P., Wexels-Riser, C., Kitidis, V., Law, C.S., Zodiatis, G., 2005. Nutrient cycling in the south east Levantine basin of the eastern Mediterranean: results from a phosphate starved system. Deep Sea Research II, this volume [doi:10.1016/j.dsr2.2005.08.009].

Law, C.S., Watson, A.J., Liddicoat, M.I., 1994. Automated vacuum analysis of sulphur hexafluoride in seawater: derivation of the atmospheric trend (1970–1993) and potential as a transient tracer. Marine Chemistry 48 (1), 57–69.

Law, C.S., Watson, A.J., Liddicoat, M.I., Stanton, T., 1998. Sulphur hexafluoride as a tracer of biogeochemical and physical processes in an open-ocean iron fertilisation experiment. Deep-Sea Research II 45 (6), 977–994.

Law, C.S., Martin, A.P., Liddicoat, M.I., Watson, A.J., Richards, K.J., Woodward, E.M.S., 2001. A Lagrangian SF_6 tracer study of an anticyclonic eddy in the North Atlantic: patch evolution, vertical mixing and nutrient supply to the mixed layer. Deep-Sea Research II 48 (4–5), 705–724.

Law, C.S., Abraham, E.R., Watson, A.J., Liddicoat, M.I., 2003. Vertical eddy diffusion and nutrient supply to the surface mixed layer of the Antarctic Circumpolar Current. Journal of Geophysical Research 108 (C8) art. no. 3272.

Li, W.K.W., Dickie, P.M., Irwin, B.D., Wood, A.M., 1992. Biomass of bacteria, cyanobacteria, prochlorophytes, and photosynthetic eukaryotes in the Sargasso Sea. Deep-Sea Research I 39, 501–519.

Martin, A.P., 2003. Phytoplankton patchiness: the role of lateral stirring and mixing. Progress in Oceanography 57, 125–174.

Martin, J.H., Coale, K.H., Johnson, K.S., Fitzwater, S.E., Gordon, R.M., Tanner, S.J., Hunter, C.N., Elrod, V.A., Nowicki, J.L., Coley, T.L., Barber, R.T., Lindley, S., Watson, A.J., Van Scoy, K., Law, C.S., et al., 1994. Testing the iron hypothesis in ecosystems of the Equatorial Pacific Ocean. Nature 371 (6493), 123–129.

Martin, A.P., Richards, K.J., Law, C.S., Liddicoat, M.I., 2001. Horizontal dispersion within an anticyclonic mesoscale eddy. Deep Sea Research II 48 (4–5), 739–756.

Nightingale, P.D., Malin, G., Law, C.S., Watson, A.J., Liss, P.S., Liddicoat, M.I., Boutin, J., Upstill-Goddard, R.C., 2000. In situ evaluation of air–sea gas exchange parameterizations using novel conservative and volatile tracers. Global Biogeochemical Cycles 14 (1), 373–387.

Pasternak, A., Wassmann, P., Riser, C.W., 2005. Does mesozooplankton respond to episodic nutrient inputs in the eastern Mediterranean? Deep Sea Research II, this volume [doi:10.1016/j.dsr2.2005.09.002].

Pitta, P., Stambler, N., Tanaka, T., Zohary, T., Tselepides, A., Rassoulzadegan, F., 2005. Biological response to P addition in the Eastern Mediterranean Sea. A race against time in the microbial side. Deep Sea Research II, this volume [doi:10.1016/j.dsr2.2005.08.012].

Psarra, S., Zohary, T., Krom, M., Mantoura, R.F.C., Polychronaki, T., Stambler, N., Tselepides, A., Thingstad, T.F., 2005. Phytoplankton response to a Lagrangian phosphate addition in the Levantine Sea (Eastern Mediterranean). Deep Sea Research II, this volume [doi:10.1016/j.dsr2.2005.08.015].

Roether, W., Manca, B., Klein, B., Bregant, D., Georgopoulos, D., Beitzel, V., Kovacevic, V., Luchetta, A., 1996. Recent changes in the Eastern Mediterranean deep waters. Science 271, 333–335.

Skellam, J.G., 1951. Random dispersal in theoretical populations. Biometrika 38, 196–218.

Stanton, T.P., Law, C.S., Watson, A.J., 1998. Physical evolution of the IronEx-I open ocean tracer patch. Deep-Sea Research II 45 (6), 947–975.

Thingstad, T.F., 2005. Simulating the response to phosphate additions in the oligotrophic eastern Mediterranean using an idealized 4-member microbial food web model. Deep-Sea Research II, this volume [doi:10.1016/j.dsr2.2005.08.017].

Thingstad, T.F., Rassoulzadegan, F., 1995. Nutrient limitations, microbial food webs, and biological C-pumps in a P-limited Mediterranean. Marine Ecology Progress Series 117 (1-3), 299–306.

Thingstad, T.F., Mantoura, R.F.C., 2005. Titrating excess-N content of P-deficient Eastern Mediterranean surface water using alkaline phosphatase activity as a bio-indicator. Limnology and Oceanography 49 (5), 1582–1592.

Thingstad, T.F., Krom, M.D., Mantoura, R.F.C., Flaten, G.A.F., Herut, B., Kress, N., Law, C.S., Pasternak, A., Pitta, V., Psarra, S., Rassoulzadegan, F., Tanaka, T., Tselipides, A., Wassmann, P., Woodward, E.M.S., Wexels-Risser, C., Zohary, T., 2005. Nature of P limitation in the ultraoligotrophic Eastern Mediterranean. Science 309 (5737), 1068–1071.

Wanninkhof, R., 1992. Relationship between wind speed and gas exchange over the ocean. Journal of Geophysical Research 97 (C5), 7373–7382.

Woodward, E.M.S., Rees, A.P., 2001. Nutrient distributions in an anticyclonic eddy in the North East Atlantic Ocean, with reference to nanomolar ammonium concentrations. Deep-Sea Research II 48, 775–794.

Woodward, E.M.S., Rees, A.P., 2002. Nanomolar detection for phosphate and nitrate using liquid waveguide technology. EOS Transactions (American Geophysical Union, supplement) 83 (4), 92.

Zodiatis, G., Drakopoulos, P., Groom, S.W., Tselepides, A., 2005. Variability of the Cyprus Warm Core Eddy before, during and after the CYCLOPS Project. Deep Sea Research II, this volume [doi:10.1016/j.dsr2.2005.08.020].

Zohary, T., Robarts, R.D., 1998. Experimental study of microbial P limitation in the eastern Mediterranean. Limnology and Oceanography 43, 387–395.

Zohary, T., Herut, B., Krom, M.D., Mantoura, R.F.C., Pitta, P., Psarra, S., Rassoulzadegan, F., Stambler, N., Tanaka, T., Thingstad, T.F., Woodward, E.M.S., 2005. P-limited but N&P co-limited phytoplankton in the Eastern Mediterranean—a microcosm experiment. Deep-Sea Research II, this volume [doi:10.1016/j.dsr2.2005.08.011].